ASSESSMENT OF TOOL NOSE WEAR USING SCANNED IMAGES OF CUTTING INSERTS

Lim Teong Yeong[1]*, Chiang Ee Pin[1] and Woo Yian Peen[2]

[1]School of Mechanical Engineering, College of Engineering, Universiti Teknologi MARA, 13500 UiTM Permatang Pauh, Pulau Pinang, Malaysia

[2]School of Civil Engineering, College of Engineering, Universiti Teknologi MARA 13500 UiTM Permatang Pauh, Pulau Pinang, Malaysia

*Corresponding email: tylim527@uitm.edu.my

ABSTRACT

The surface quality of final product in machining is governed by many intimately related factors such as tool conditions and machining parameters. Amongst these factors, tool wear is essentially one of the most prominent influences on dimensional accuracy, surface roughness and tool life. Since the measurement of tool wear in manufacturing is still done manually, automated and intelligent measurement of wear are gaining more interest in the perspective of reducing human interference and hence, the accurate assessment of tool condition. This research work proposes a fast and reliable image processing method in measuring the nose wear of cutting inserts. Two image digitization methods were used, which are flatbed scanner (CanoScan5600F) and 3-D metrology system (Alicona InfiniteFocus). A sub-pixel edge detection algorithm was developed in the segmentation of nose area to improve the measurement accuracy. Scanning of tool nose was conducted before and after the machining for the measurement of wear area. Results show that about 5% to 6% of average absolute deviations were obtained from the measurement of nose wear area (A_p)and nose flank wear ($VB_{c(max)}$) using images from InfiniteFocus and scanner.

Keywords: *Tool Wear, Machine Vision, Image Processing*

1.0   INTRODUCTION

In manufacturing systems, estimation of cutting tool life under given cutting conditions is important yet complex problems due to the nature of tool kind selected in different cutting processes [1]. The level of tool wear is one of the most important tool life indicators and must be measured as accurately as possible because the quality of the machining output such as surface quality and dimension is directly correlated to the tool conditions. The tool wear, specifically the nose wear, is one of the critical wear regions in determining the surface quality because it shortens the cutting tools and increases gradually the dimension of machined surface, thus introducing significant dimensional errors which could reach 0.03 mm - 0.05 mm [2]. In machining, there are basically three wear zones of a cutting insert according to its principal location on a cutting tool which are crater wear, flank wear and nose wear as illustrated in Figure 1. The nose wear, which generally consist of many combinations of wear along the nose edge, is the most noticeable type of wear that occurs because of the direct interaction of the tool nose with the machined parts as well as the chips formed during machining. In the economic perspective manufacturers are also facing the challenge of deciding the optimal intervals [3] to replace or recondition their tools, in corresponding to quality, cost and productivity. Thus, determining the tool wear is essentially crucial in the metal cutting industry. Generally, tool wear monitoring is either direct measurement using optical microscope or

camera, or measured indirectly using force, surface finish or temperature which are affected by tool wear [4]. However, direct measurement using machine vision and image processing techniques has gained more interest due to its flexibility that offers fast and comparatively more accurate methods with the option of automation and algorithms. The nature of machine vision inspection which is non-contact and non-destructive are important characteristics of machine vision process. The integration between both hardware and software by automation further extent the capability of feature extraction and recognition, which makes the system nowadays more intelligent in decision making [5].
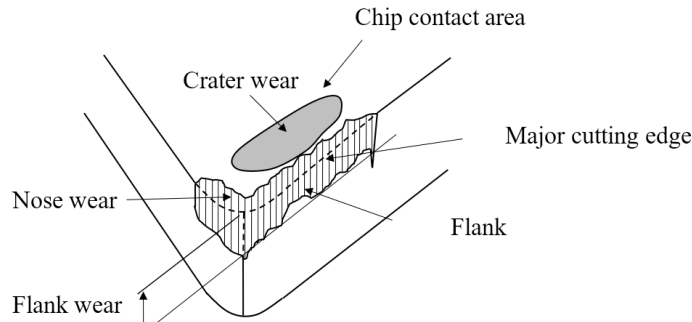

Figure 1: Typical cutting tool wear [5]

Extensive study has been made in monitoring tool wear using machine vision for various kinds of cutting operation [6-10, 12-15]. However, research communities are still giving more attention to wear detection based on extracted features using highly sophisticated camera devices or scopes. This study aims at researching a low-cost yet reliable and high accuracy digitization approach (flatbed scanner) in wear measurement. The turning cutting inserts (positive tool) were used in the study of developing tool wear measurement algorithm. To determine the accuracy of the proposed method, the 3-D metrology measurement system (*Alicona InfiniteFocus*) was used for comparison of measurement results.

2.0   METHODOLOGY

2.1   Definition of Nose Wear of Positive Inserts

A typical difference between positive and negative inserts is illustrated in Figure 2(a)-(b). A negative insert has an angle of 90° (0° clearance angle), while a positive insert has an angle of less than 90° (7° clearance angle). The positive insert is normally single sided with low cutting forces which are normally used for internal turning and external turning of slender components. Negative insert has double or single-sided cutting tips. It has zero clearance and thus gives high edge strength and is normally used in heavy machining. For positive inserts, two parameters of nose wear are defined, namely projected nose wear area, Ap and maximum nose flank wear, $VB_{c(max)}$. The projected nose wear area, Ap is the area between the worn and the unworn nose edges as shown in Figure 3.
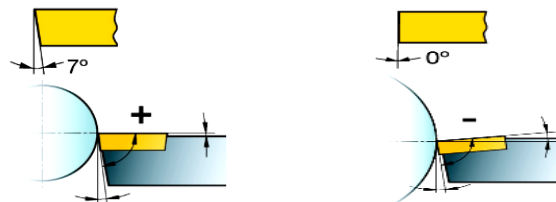

Figure 2. Illustration of (a) positive insert and (b) negative insert mounted on a tilted tool holder [11]

The relief angle can be obtained from the manufacturer catalogue. To obtain $VB_{c(max)}$, the nose flank wear VB_c, is first derived:

$$VB_c = \frac{t_i}{\tan \theta_r} \tag{1}$$

where t_i is the projection length between the worn and the unworn nose edge. The maximum value of h_i denotes the $VB_{c(max)}$ which occurs in any location on the worn edge. Hence, $VB_{c(max)}$ is defined as:

$$VB_{c(max)} = \max(VB_c) \tag{2}$$
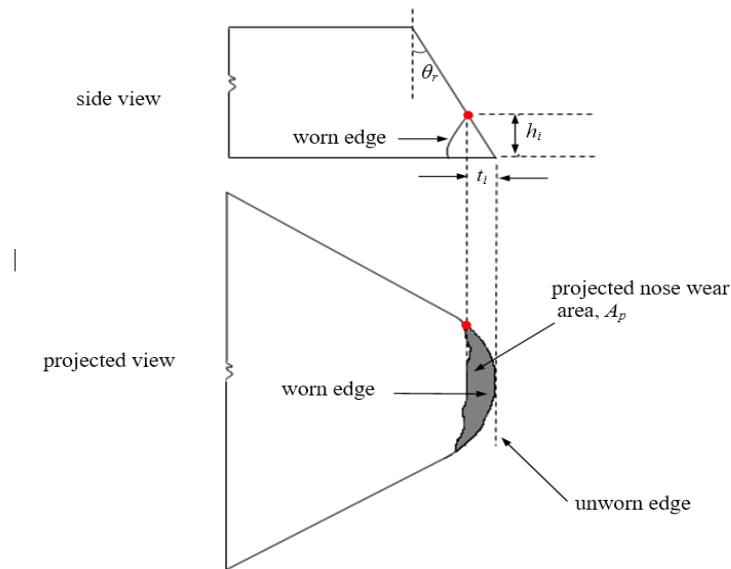
Figure 3. Nose wear measurement of cutting inserts

## 2.2   Machining Conditions for Positive Inserts

As stated in many published literatures, tool wear is affected by various machining conditions such as machining time, machining speed, feed rate and tool material. In this study, cutting speed and machining time were used to study the effectiveness of the flatbed scanner to measure tool wear of inserts. Detailed machining parameters are shown in Table 1. The machining conditions were chosen arbitrary with the primary objective to obtain progressing wear patterns. The selected machining time, speeds and depth of cut were used to prevent excessive machining which can cause tool breakage. For various machining time from 5 minutes to 30 minutes, cutting speed of 42.5 mm/min was used. All machining work were conducted using conventional lathe (Pinocho 290/200 (Italy)) using uncoated cemented carbide inserts with nominal nose radius of 0.800 mm and 0.400 mm which were commonly used in machining.

## 2.3   Image Acquisition of Tools

Several cutting tool inserts of different shapes and radii manufactured by Sandvik Coromant Ltd. (Sweden) were scanned using the flatbed scanner. These are 0.4 mm radius triangular inserts (TPUN 16-03-04, CNMG 12-04-04), 0.4 mm radius square insert (SPUN 12-03-04), 0.4 mm radius rhombic insert (CNMG 12-04-04). The tool was scanned and saved using *ArcSoft PhotoStudio5* from *Canon* commercial imaging scanner (Canoscan 5600F) as shown in Figure 4 for an open scanning. The ArcSoft PhotoStudio5 was used in all images capturing involving scanner whereas Matlab Image Processing toolbox was used in all the image processing.

Table 1. Machining conditions for positive inserts

Machine Tool	Conventional lathe (Pinocho 290/200 Italy)
Work piece	Stainless steel rod, AISI308
Cutting Tools	Uncoated cemented carbide: TPMN160308 UX30
Feed rate	0.081 mm/rev
Machining time	5, 10, 15, 20, 25 and 30 mins
Cutting speed	42.5 mm/min
Depth of cut	0.5 mm
Coolant	Air
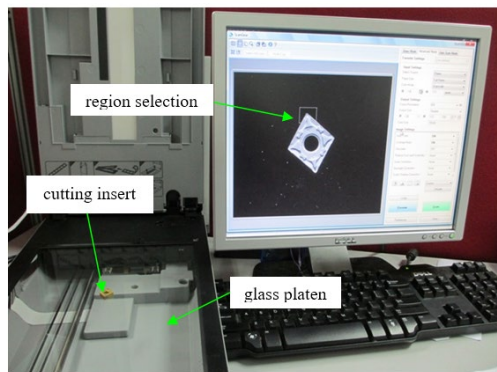
**Figure 4.** Scanning of individual insert using *ArcSoft PhotoStudio5*
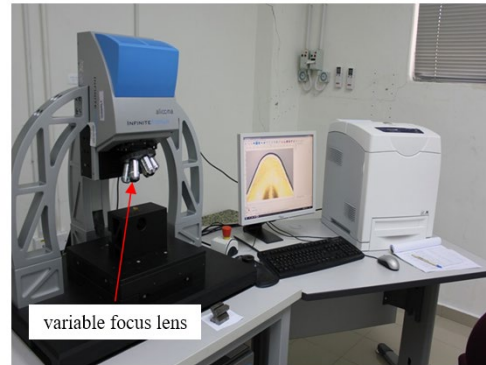
Figure 5. Scanning of individual insert using *Alicon InfiniteFocus*

The whole insert was first previewed on the scanner and was followed by the selection of ROI with the available zoom-in feature. The processor used in developing the scanning and processing of insert images is Dell Intel®Core™ i5-3470 CPU @3.2 GHz with 64 bit OS, x64 based processor. To verify the measurement results obtained using flatbed scanner, a commercial high magnification focus variation 3-D metrology system (*Alicona InfiniteFocus*) was used to capture the images of the inserts. The tool was illuminated by the modulated light. This light is transmitted through the optic and is focused through a beam splitter onto the specimen. The digital sensor receives the projected light by the light reflected from the tool. The *Alicona InfiniteFocus* as shown in Figure 5 is capable of measuring the small radius of the tool tip. The tip of each tool insert was placed on the scanning stage and was scanned one at a time. The scanning was conducted using a magnification of 10X and a resolution of 1.75 *μ*m/pixel using the variable focus lens. The distance of the lens on top of the tool was adjusted manually using the panel for the best sharpness view of the tool tip on the monitor before scanning. After acquiring the image, the measurement of nose radii was carried out in the software provided in *InfiniteFocus* using the multiple points' radius estimation function.

2.4   Image Processing Algorithms

For the measurement of nose wear, the images of inserts were first scanned before machining. Two controlled lighting conditions were used to capture the insert images namely, front lighting and back lighting[5]. Each insert was then subjected to a turning process for various cutting conditions as specified in Section 2.3. After machining the insert was scanned again to obtain the wear image of worn insert. Both images were subjected to the image processing algorithm shown in Figure 6 to calculate the nose wear. The images were first filtered using 5×5 median filtering to filter the global noise in the images. Thresholding using Otsu's method was employed to binarize the filtered images. After binarization, small particles, which appear as blobs on the binary image due to heavy dust or foreign matters were eliminated. The elimination starts with labeling the blobs within the tool region followed by measuring their respective area. The tool area is very large as compared to the blobs and thus they can be identified by a small preset pixel area value. The nose sectors were

then extracted for both original and unworn images. After determining the actual nose segment (coordinates between *P* and *Q*) and the exact nose center *R*, the images of worn and unworn tool were then rotated in order to obtain properly aligned scanned images before and after machining. The angle of rotation θ_p is determined by calculating the angle between the fitted lines to the vertical as shown in Figure 7(a). After rotation (Figure 7(b)) the points *P*, *Q* and *R* are shifted to *P′*, *Q′* and *R′* respectively using the MATLAB 'imrotate' command from image processing toolbox where the command rotates image by angle degrees in a counterclockwise direction around the center point of image (Mathworks Inc., 2005). Next, auto-cropping process was applied in order to extract a smaller region for polar radius transformation.
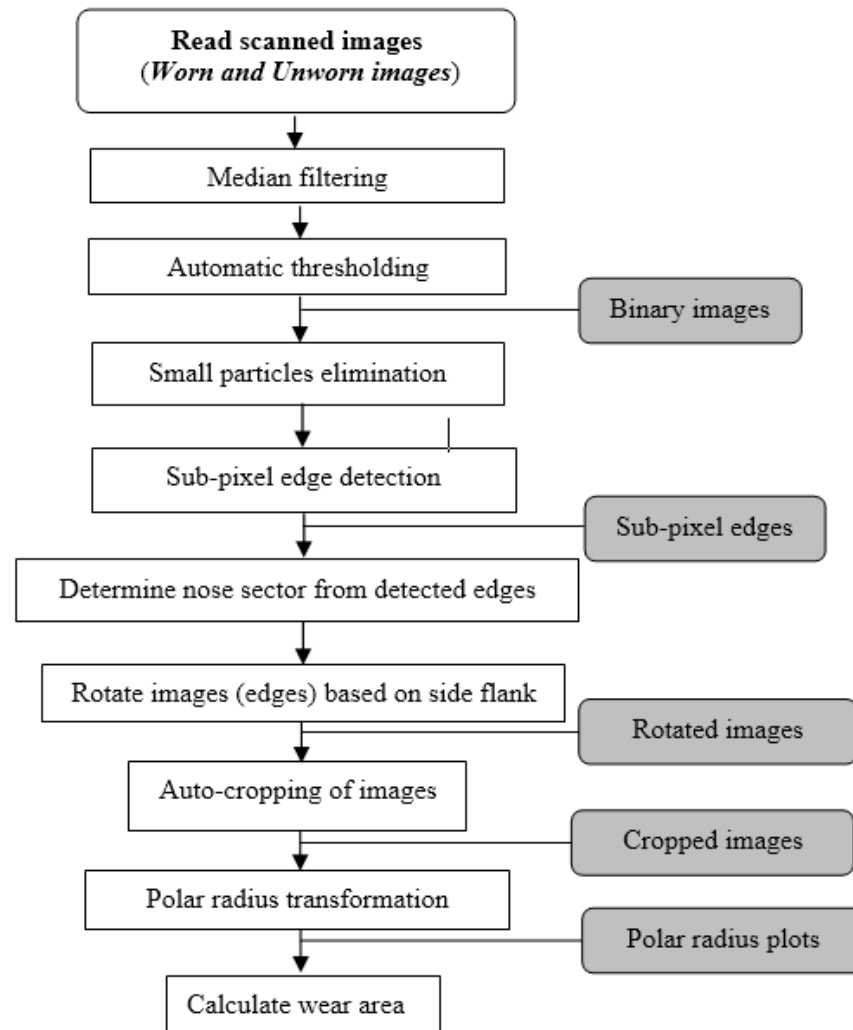
Figure 6. Flowchart of nose wear area calculation of cutting insert.

(a)

(b)

(c)
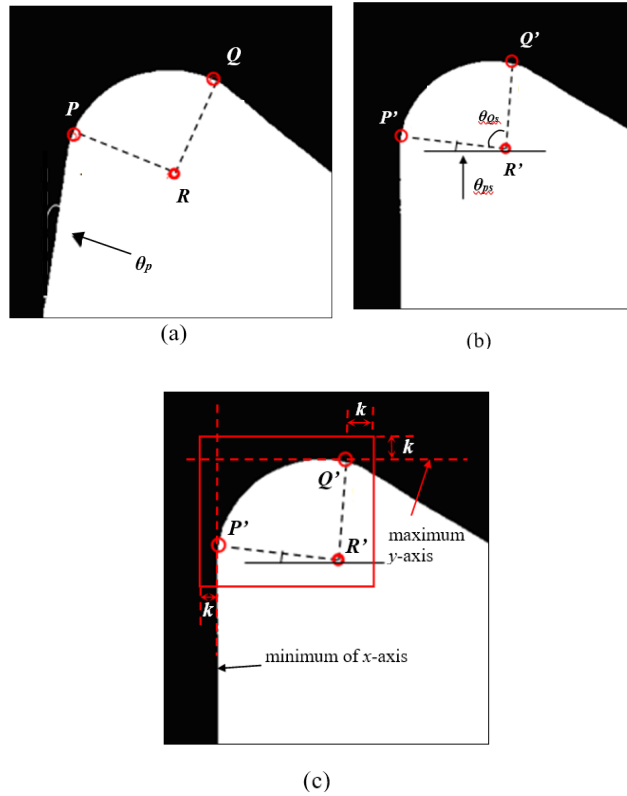
**Figure 7**. (a) Detected nose segment and (b) rotated nose segment (c) cropped region of an unworn insert.

The auto cropping process was carried out by referring to the left most side edge of the tool (minimum x-axis), the maximum y-axis and the point R' of the image as shown in Figure 7(c). A preset distance of k was set to crop the image. To determine the center for polar radius transformation for both worn and unworn images, the exact circle center detected for unworn image was used as the reference.

2.5   Polar Radius Transformation

Polar radius transformation was used to transform all the edge coordinates on the nose sector into radius (distance from tool/circle center (sub-pixels)) versus the corresponding angles as illustrated in Figure 8 and Figure 9 for the unworn and worn insert respectively. The area of a sector is given by:

$$Area = \frac{\theta}{360}\pi r^{2}$$

(3)

where r is the radius and θ is the angle in degree.
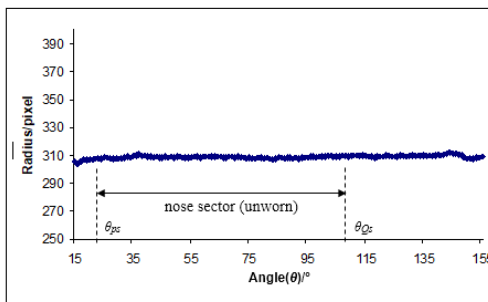
Figure 8: Flowchart of nose wear area calculation of cutting insert.
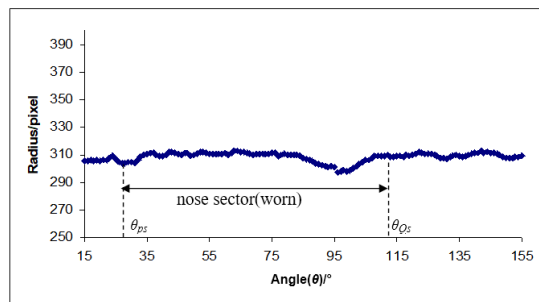
Figure 9: Flowchart of nose wear area calculation of cutting insert.

Thus, from the polar plot, the sub-pixel nose wear area in pixels is calculated as:

$$Area(pixel) = \sum_{i=1}^{N-1} \left(\pi \left[\frac{\theta_{i+1} - \theta_n}{360} \right] \left((r_{1i})^2 - (r_{2i})^2 \right) \right) \tag{4}$$

where N corresponds to the total number of sub-pixel points involved within the nose segment, r_1 and r_2 are radii for worn and unworn inserts, θ is the angle in degree. The metric measurement of projected nose wear area, A_p from scanning resolution of dpi unit can be obtained by using the average scaling factor SF_{avg}:

$$A_p(mm^2) = Area(pixel) \times \left(\frac{25.4}{SF_{avg}(dpi)} \right)^2 \tag{5}$$

For nose flank wear, VB_c the projection length t_i is substituted with radii r_{1i} and r_{2i}:

$$VB_c(pixel) = \frac{r_{1i} - r_{2i}}{\tan \theta_r} \tag{6}$$

Hence, the metric measurement of $VB_{c(max)}$ using scanning resolution of dpi unit and scaling factor, SF_{avg} is given by:

$$VB_{c(max)}(mm) = VB_{c(max)}(pixel) \times \frac{25.4}{SF_{avg}(dpi)} \tag{7}$$

The same image processing algorithm methodology was applied to images obtained from *InfiniteFocus* and the nose wear was then calculated and compared with the measurement obtained from scanned images using flatbed scanner.
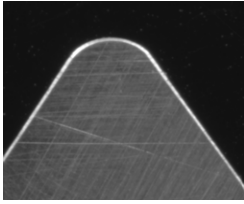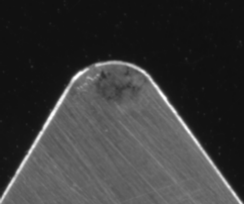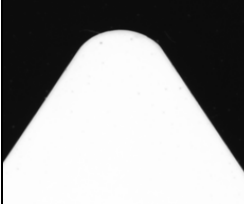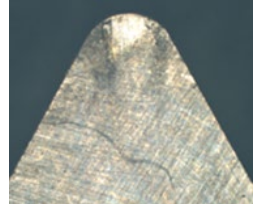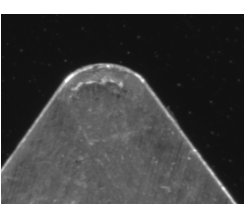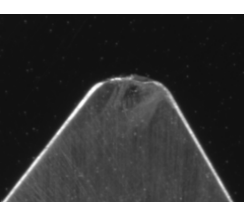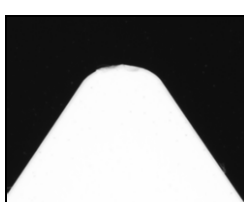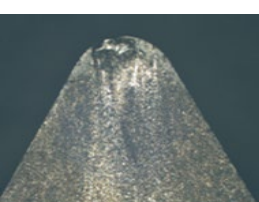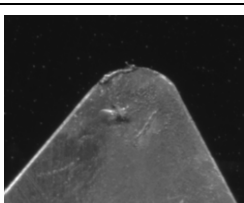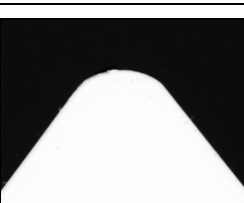
3.0 RESULTS AND DISCUSSIONS

From the images in Table 2, it is found that backlight scanning produces good contrast as the edge of the insert is clearly distinguished from the background. This is followed by front lighting though overexposure causes bright spots along the edges.

The *InfiniteFocus* system gives the lowest contrast due to the localized directional spot illumination on the tool nose which causes low contrast zone to occur especially along the edges. The nose wear area, A_p measured is shown in Table 3. The maximum absolute deviation between backlight scanning and *InfiniteFocus* system, and front light scanning and *InfiniteFocus* system are 8.29% and 11.06% respectively. Generally, back light scanning yields lower wear difference compared to front light scanning with the average overall absolute deviation of 4.49% and 7.54% respectively.

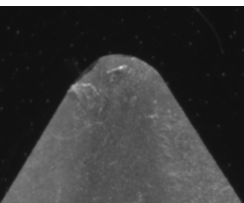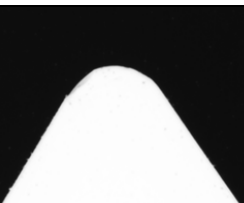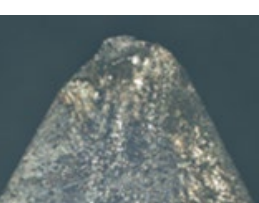Besides that, the back light scanning has a slight tendency to underestimate the wear (average deviation of 0.49%) as compared to *InfiniteFoucus* whereas front light tends to overestimate (average deviation of -0.93%). Also, the back light scanning gives lower uncertainty as compared to front light scanning, in terms of deviation. Figure 10 shows the comparison of wear area in millimeter square for various scanning conditions. As expected, the wear area increases with the increase of machining time. Front light scanning yields higher overall wear area as compared to measurement using back light scanning and *InfiniteFocus* system after 15 minutes of machining.

Table 2: Scanned images.

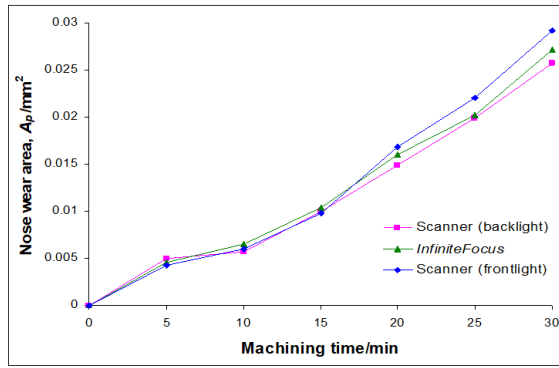| Cutting time (min)	Scanner (Frontlight)	Scanner (Backlight)	*InfiniteFocus*
0			
5			
10			
15			
25			
30			

Table 3: Nose wear area A_p measurement using different cutting time.

Cutting time (min)	Detected nose wear area, A_p (mm^2)			Deviation (%)		Absolute deviation (%)	
	Scanner (BL)	Scanner (FL)	*IFocus*	Scanner (BL) Vs *IFocus*	Scanner (FL) Vs *IFocus*	Scanner (BL) Vs *IFocus*	Scanner (FL) Vs *IFocus*
5	0.0050	0.0043	0.0046	-8.29	6.85	8.29	6.85
10	0.0062	0.0060	0.0065	4.28	7.58	4.28	7.58
15	0.0100	0.0098	0.0104	3.91	5.41	3.91	5.41
20	0.0166	0.0169	0.0160	-3.70	-5.31	3.70	5.31
25	0.0199	0.0221	0.0202	1.62	-9.05	1.62	9.05
30	0.0258	0.0302	0.0272	5.12	-11.06	5.12	11.06
AVERAGE				0.49	-0.93	4.49	7.54
SD				5.35	8.50	2.19	2.22
Uncertainty				±5.62	±8.91	±2.30	±2.33

Table 4: Maximum nose flank wear measurement, $VB_{c(max)}$ using different cutting time

Cutting Time (min)	Detected maximum nose flank wear, $VB_{c(max)}$ (mm)			Deviation (%)		Absolute deviation (%)	
	Scanner (BL)	Scanner (FL)	*IFocus*	Scanner (BL) Vs *IFocus*	Scanner (FL) Vs *IFocus*	Scanner (BL) Vs *IFocus*	Scanner (FL) Vs *IFocus*
5	0.1490	0.1335	0.1344	-10.86	0.67	10.86	0.67
10	0.1650	0.1550	0.1628	-1.37	4.77	1.37	4.77
15	0.1854	0.1764	0.1799	-3.06	1.95	3.06	1.95
20	0.1793	0.1733	0.1697	-5.68	-2.14	5.68	2.14
25	0.1693	0.1825	0.1725	1.88	-5.80	1.88	5.80
30	0.1663	0.1699	0.1825	8.90	6.90	8.90	6.90
AVERAGE				-1.70	1.06	5.29	3.71
SD				6.74	4.61	3.90	2.47
Uncertainty				±7.07	±4.83	±4.10	±2.59

Figure 10: Comparison of wear area *Ap* measurement using scanner and *Alicona InfiniteFocus* system using different machining time
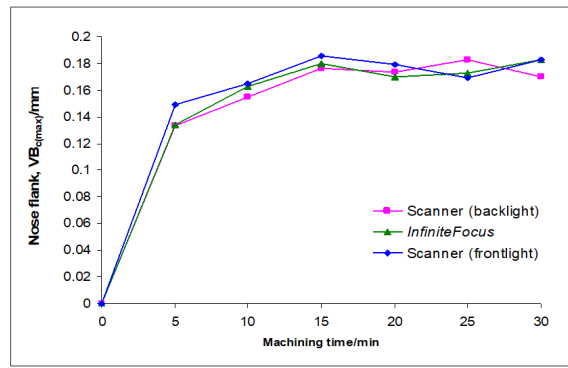
Figure 11: Comparison of maximum nose flank wear, $VB_{c(max)}$ measurement using scanner and *InfiniteFocus* system using different machining time

For images obtained using *InfiniteFocus* system, image filtering, noise and blobs elimination have to be conducted before the nose area can be extracted as heavy noise was found on the tool surface. The global value for Otsu's thresholding to obtain the binary image has to be adjusted manually to get the preferable segmentation result (Figure 12(a)-(b)). For blobs appearing after filtering, blobs elimination algorithm was used to get the final segmentation results as shown in Figure 12(a)-(c). The final image was then subjected to sub-pixel edge detection to auto detect the edge pixels and nose region. The image preprocessing on images obtained from *InfiniteFocus* system indirectly affect the accuracy of the edges obtained.

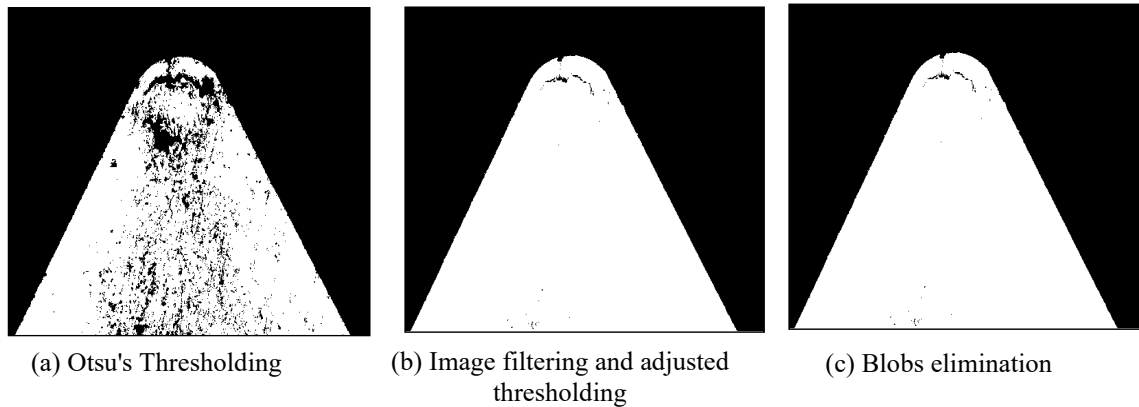(a) Otsu's Thresholding   (b) Image filtering and adjusted thresholding   (c) Blobs elimination

Figure 10 (a)-(c) Processing of images obtained from Alicona InfiniteFocus system

Besides that, the back light scanning has a slight tendency to underestimate the wear (average deviation of 0.49%) as compared to *InfiniteFoucus* whereas front light tends to overestimate (average deviation of -0.93%). Also, the back light scanning gives lower uncertainty as compared to front light scanning, in terms of deviation.

The measurement of maximum nose flank wear, $VB_{c(max)}$ is shown in Table 4. In contrast to the projected wear area A_p, the back light scanning tends to have slight overestimation if compared to front light with the average deviation of -1.70% and 1.06% respectively. Back light scanning also yields larger range of deviation, higher absolute deviation with higher uncertainty. This may due to the single value of $VB_{c(max)}$ detected from the nose edge and was used for the derivation of $VB_{c(max)}$,which as compared to the nose wear A_p, where all the values of the sub-pixels along the nose edge were transformed (to polar radius) and summed and is likely to cause less deviation. Figure 11 shows the comparison of $VB_{c(max)}$ for the three scanning methods. The $VB_{c(max)}$ values are more fluctuated as compared to A_p. The fluctuation is more noticeable after 15 minutes of machining.

Overall, the front light scanning yields highest measurement values except for the machining time at 25 minutes.

4.0   CONCLUSION

For the measurement of nose wear of positive inserts, a maximum absolute deviation of about 6% was found on the measurement of projected nose wear area (A_p) and maximum nose flank wear ($VB_{c(max)}$) based on different machining conditions. A larger variation of measurement was found for $VB_{c(max)}$ and the images obtained from the scanner have the tendency of underestimation of the maximum nose flank. For negative inserts, the reduction factor used for error compensation of nose wears calculation was estimated from the scanning of inserts on various angles. The accuracy of the factor was verified by the repeated measurement of nose wear at different machining condition and angles. About 5% to 6% of average absolute deviations were obtained from the measurement of A_p and $VB_{c(max)}$ using images from *InfiniteFocus* and scanner. No bias was found in both scanning methods, and the possibility of over/underestimation is lower as compared to positive inserts due to higher auto-focus resolution (1.75 microns/pixel) was used in *InfiniteFocus* in image acquiring.

ACKNOWLEDGEMENTS

REFERENCES

1. Addona, D.M.D, Teti R, *Image data processing via neural networks for tool wear prediction*, 8th CIRP Conference on Intelligent Computation in Manufacturing Engineering. Procedia CIRP, 2013, **12**: p252 – 257.
2. Marinov, V.   *Tool Wear and Tool Life* . Manufacturing Lecture Notes. Retrieved from https://nkumbwa.weebly.com/uploads/3/7/1/6/3716285/tool_wear_tool_life.pdf, 2005 (Accessed 12 June 2024).
3. Schlegel, C., Dirk Molitor, D.A., Kubik, C., Martin, D.M., Groche, P., *Tool wear segmentation in blanking processes with fully convolutional networks based digital image processing*, Journal of Materials Processing Tech.2024, **324**: p118270.
4. Bagga, P.J. and Makhesana, M.A, Patel, K, Tool *wear monitoring in turning using image processing techniques*, Materials Today: Proceedings, 2021, **44**: p771–775.
5. Lim, T.Y., *Measurement of Nose Radius And Wear Of Multiple Cutting Tool Inserts From 2-D Scanned Images with Sub-pixel Edge Detection*. PhD Thesis, 2015.
6. Korkmaz, M. E, Gupta, M,K., Çelik, E., Ross, N, S, Günay, M, *Tool wear and its mechanism in turning aluminum alloys with image processing and machine learning methods*. Tribology International 2024, **191**:p109-207
7. Hrechuk, A., Bushlya, *Automated detection of tool wear in machining and characterization of its shape Wear*, 2023, **523**:p204762.
8.   Zhou X,Yu., T, Wang G, Guo, R, Fu, Y., Sun, Y., Chen, M., *Tool wear classification based on convolutional neural network and time series images during high precision turning of copper Wear*, 2023, **522**:p204692
9. Holst, C., Yavuz, T.B., Gupta, P., Ganser, Bergs, T, *Deep learning and rule-based image processing pipeline for automated metal cutting tool wear detection and measurement*, IFAC Papers OnLine ,2022, **55-2**: p534–539
10. Wear analysis in cutting tools by the technique of image processing with the application of two dimensional matrices To cite this article: J H Arévalo-Ruedas et al 2021 J. Phys.: Conf. Ser. 2139 012018
11. Sandvik Coromant (2013). *How to achieve good component quality by turning: positive and negative*. Retrieved from https://www.sandvik.coromant.com/en-us/knowledge/general-turning/how-to-achieve-good-component-quality-in-turning (Accessed 12 June 2024).
12. Castejon, M., Alegre, E., Barreiro, J., & Hernandez, L. K. *On-line tool wear monitoring using geometric descriptors from digital images*. International Journal of Machine Tools and Manufacture, 2007, **12**:47, p1847-1853.
13. Chai, O. H., Wong, Y. S., & Poo, A. N. *An interpolation scheme for tool-radius compensated parabolic paths for CNC. IIE transactions*, 1996, **1**:28, p11-17.
14. Chen, S. K., & Hollender, L. *Digitizing of radiographs with a flatbed scanner*. Journal of dentistry, 1995, **4**:23, p205-208.
15. Chian, G. J., & Ratnam, M. M. *Determination of tool nose radii of cutting inserts using machine vision*. Sensor Review, 2011, **2**:31, p127-137.